

Vacuum Stability of Standard Model⁺⁺

Luis A. Anchordoqui,¹ Ignatios Antoniadis,^{2,*} Haim Goldberg,³
Xing Huang,⁴ Dieter Lüst,^{5,6} Tomasz R. Taylor,³ and Brian Vlcek¹

¹*Department of Physics,
University of Wisconsin-Milwaukee, Milwaukee, WI 53201, USA*

²*Department of Physics,
CERN Theory Division, CH-1211 Geneva 23, Switzerland*

³*Department of Physics,
Northeastern University, Boston, MA 02115, USA*

⁴*School of Physics and Astronomy,
Seoul National University, Seoul 151-747, Korea*

⁵*Max-Planck-Institut für Physik,
Werner-Heisenberg-Institut, 80805 München, Germany*

⁶*Arnold Sommerfeld Center for Theoretical Physics
Ludwig-Maximilians-Universität München, 80333 München, Germany*

Abstract

The latest results of the ATLAS and CMS experiments point to a preferred narrow Higgs mass range ($m_H \simeq 124 - 126$ GeV) in which the effective potential of the Standard Model (SM) develops a vacuum instability at a scale $10^9 - 10^{11}$ GeV, with the precise scale depending on the precise value of the top quark mass and the strong coupling constant. Motivated by this experimental situation, we present here a detailed investigation about the stability of the SM⁺⁺ vacuum, which is characterized by a simple extension of the SM obtained by adding to the scalar sector a complex $SU(2)$ singlet that has the quantum numbers of the right-handed neutrino, H'' , and to the gauge sector an $U(1)$ that is broken by the vacuum expectation value of H'' . We derive the complete set of renormalization group equations at one loop. We then pursue a numerical study of the system to determine the triviality and vacuum stability bounds, using a scan of 10^4 random set of points to fix the initial conditions. We show that, if there is no mixing in the scalar sector, the top Yukawa coupling drives the quartic Higgs coupling to negative values in the ultraviolet and, as for the SM, the effective potential develops an instability below the Planck scale. However, for a mixing angle $-0.35 \lesssim \alpha \lesssim -0.02$ or $0.01 \lesssim \alpha \lesssim 0.35$, with the new scalar mass in the range $500 \text{ GeV} \lesssim m_{h''} \lesssim 8 \text{ TeV}$, the SM⁺⁺ ground state can be absolutely stable up to the Planck scale. These results are largely independent of TeV-scale free parameters in the model: the mass of the non-anomalous $U(1)$ gauge boson and its branching fractions.

*On leave of absence from CPHT Ecole Polytechnique, F-91128, Palaiseau Cedex.

Contents

I. Introduction	2
II. RG Evolution Equations of SM ⁺⁺	3
III. Results and Conclusions	9
Acknowledgments	15
References	16

I. INTRODUCTION

The CERN Large Hadron Collider (LHC) has begun a bound and determined exploration of the electroweak scale. Recently, the ATLAS [1] and CMS [2] collaborations presented an update of the Higgs searches, independently combining about 5 fb^{-1} of data collected at $\sqrt{s} = 7 \text{ TeV}$ and more than 5 fb^{-1} at $\sqrt{s} = 8 \text{ TeV}$. The excess at 125 GeV that was evident already in data from the 7 TeV run [3, 4] has been consistently observed by both experiments in the $\gamma\gamma$ invariant mass spectrum with a local significance of 4.5σ and 4.1σ , respectively. In addition, an excess of 4 leptons events (with $m_{4\ell} \simeq 125 \text{ GeV}$) which can be interpreted as a signal of the $H \rightarrow ZZ^* \rightarrow 4\ell$ decay, is observed by both experiments with a significance of 3.4σ and 3.2σ , respectively. The CMS experiment also presented updated Higgs boson searches in W^+W^- (a broad excess in the invariant mass distribution of 1.5σ is observed), $b\bar{b}$ (no excess is observed), and $\tau\bar{\tau}$ (no excess is observed) channels. More recently, the ATLAS Collaboration reported a 2.8σ deviation in the $H \rightarrow W^+W^- \rightarrow 2\ell\nu$ decay channel [5]. When combining the data from the 7 TeV and 8 TeV runs, both experiments separately have reached the sensitivity to the new boson with a local significance of 5σ [6, 7]. Very recently, the CDF and D0 collaborations published an update on searches for the Higgs boson decaying into $b\bar{b}$ pairs, using 9.7 fb^{-1} of data collected at $\sqrt{s} = 1.96 \text{ TeV}$ [8]. They reported a 3.3σ deviation with respect to the background-only hypothesis in the mass range between 120 – 135 GeV.

All in all, LHC data strongly suggest that the observed state feeds the electroweak symmetry breaking, and is likely the Higgs boson. However, it remains to be seen whether its trademarks, particularly the production cross section and decay branching fractions, agree with the very precise prediction of the Standard Model (SM). The decay channels that are most sensitive to new physics are the loop induced decays $H \rightarrow \gamma\gamma$ and $H \rightarrow \gamma Z$. Interestingly, the most recent analyses [9, 10] of the combined LHC data seem to indicate that there is a deviation from SM expectations in the diphoton channel at the $2.0\sigma - 2.3\sigma$ level; see, however, [11].

From a theoretical perspective some modification of the Higgs sector has long been expected, since the major motivation for physics beyond the SM is aimed at resolving the hierarchy problem. Even if one abandons such a motivation for new physics there are still enduring concerns about the stability of the electroweak vacuum, which have been exacerbated by the new LHC data that points to $m_H \simeq 125 \text{ GeV}$.

Next-to-leading order (NLO) constraints on SM vacuum stability based on two-loop renormalization group (RG) equations, one-loop threshold corrections at the electroweak scale

(possibly improved with two-loop terms in the case of pure QCD corrections), and one-loop effective potential seem to indicate $m_H \approx 125 - 126$ GeV saturates the minimum value that ensures a vanishing Higgs quartic coupling around the Planck scale (M_{Pl}), see *e.g.* [12–22, 44]. However, the devil is in the details, a more recent NNLO analysis [23, 24] yields a very restrictive condition of absolute stability up to the Planck scale

$$m_H > \left[129.4 + 1.4 \left(\frac{m_t/\text{GeV} - 173.1}{0.7} \right) - 0.5 \left(\frac{\alpha_s(m_Z) - 0.1184}{0.0007} \right) \pm 1.0_{\text{th}} \right] \text{ GeV}. \quad (1)$$

When combining in quadrature the theoretical uncertainty with experimental errors on the mass of the top (m_t) and the strong coupling constant (α_s), one obtains $m_H > 129 \pm 1.8$ GeV. The vacuum stability of the SM up to the Planck scale is excluded at 2σ (98% C.L. one sided) for $m_H < 126$ GeV [23, 24]. Achieving the stability will necessarily impose constraints on physics beyond the SM.

Very recently we have put forward a (string based) Standard-like Model [25]. Motivated by the above, here we study the vacuum stability of its scalar sector. The layout of the paper is as follows. In Sec. II we briefly review the generalities of our model and we derive the RG equations. In Sec. III we present our results and conclusions.

II. RG EVOLUTION EQUATIONS OF SM⁺⁺

Very recently, we engineered the minimal extension of the SM that can be embedded into a Superstring Theory endowed with a high mass string scale, $M_s \lesssim M_{\text{Pl}}$ [25]. The gauge extended sector, $U(3)_B \times SU(2)_L \times U(1)_{I_R} \times U(1)_L$, has two additional $U(1)$ symmetries and thus we refer to our model as SM⁺⁺. The origin of this model is founded on the D-brane structure of string compactifications, with all six extra dimensions $\mathcal{O}(M_{\text{Pl}}^{-1})$ [26–28]. The low energy remnants of the D-brane structure are the gauge bosons and Weyl fermions living at the brane intersections of a particular 4-stack quiver configuration [29]. A schematic representation of the D-brane construct is shown in Fig. 1. The general properties of the chiral spectrum are summarized in Table I.

The resulting $U(1)$ content gauges the baryon number B [with $U(1)_B \subset U(3)_B$], the lepton number L , and a third additional abelian charge I_R which acts as the third isospin component of an $SU(2)_R$. Contact with gauge structures at TeV energies is achieved by a field rotation to couple diagonally to hypercharge Y_μ . Two of the Euler angles are determined by this rotation and the third one is chosen so that one of the $U(1)$ gauge bosons couples only to an anomaly free linear combination of I_R and $B - L$. Of the three original abelian couplings, the baryon number coupling g'_3 is fixed to be $\sqrt{1/6}$ of the QCD coupling g_3 at the string scale. The orthogonal nature of the rotation imposes one additional constraint on the remaining couplings g'_1 and g'_4 [30]. Since one of the two extra gauge bosons is coupled to an anomalous current, its mass is $\mathcal{O}(M_s)$, as generated through some Stückelberg mechanism.¹ The other gauge boson is coupled to an anomaly free current and therefore (under certain

¹ A point worth noting at this juncture: SM can also be embedded in a 3-stack quiver comprising (only) one additional $U(1)$ symmetry, $U(3) \times SU(2) \times U(1)$ [31]. The extra gauge boson is anomalous and must grow a Stückelberg mass $\sim M_s$. In this D-brane model the running of the quartic Higgs coupling would reveal a vacuum instability around 10^{10} GeV [23, 24].

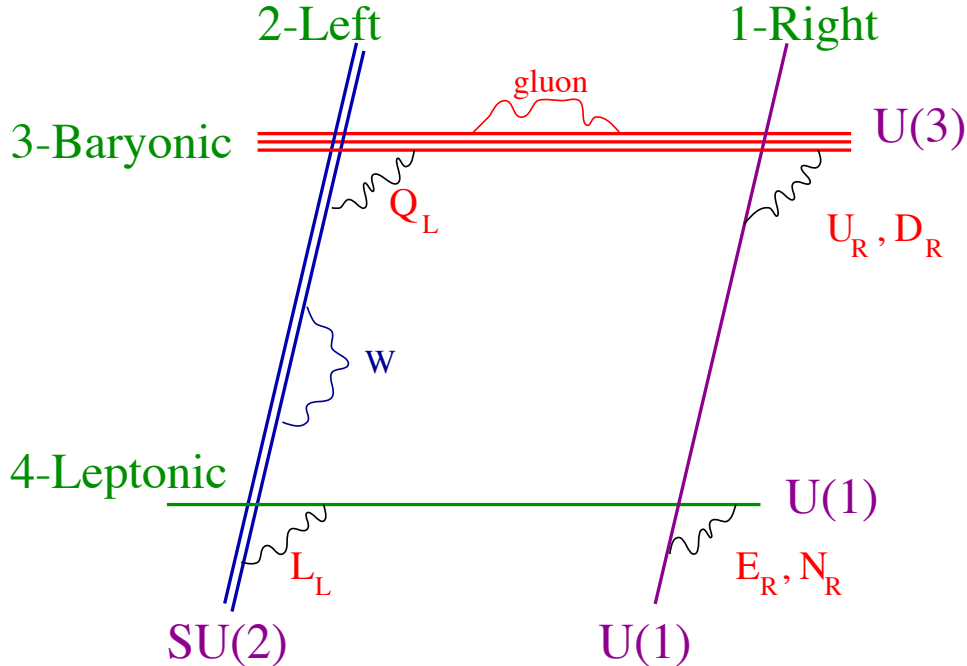


FIG. 1: Pictorial representation of the $U(3)_B \times SU(2)_L \times U(1)_L \times U(1)_{I_R}$ D-brane model.

topological conditions) it can remain massless and grow a TeV-scale mass through ordinary Higgs mechanisms [32].

Electroweak symmetry breaking is achieved through the standard Higgs doublet H . The spontaneous symmetry breaking of the extra non-anomalous $U(1)$ is attained through an $SU(2)$ singlet scalar field H'' , which carries L and I_R numbers, and acquires a vacuum expectation value (VEV) at the TeV scale. With the charge assignments of Table I there are no dimension 4 operators involving H'' that contribute to the Yukawa Lagrangian. This is very important since H'' carries the quantum numbers of right-handed neutrino and its VEV breaks lepton number. However, this breaking can affect only higher-dimensional operators which are suppressed by the high string scale, and thus there is no phenomenological problem with experimental constraints for M_s higher than $\sim 10^{14}$ GeV. Herein we remain agnostic with respect to supersymmetry (SUSY) breaking and the details of the low energy effective potential. However, we do subject the choice of quantum numbers for H'' to the stringent holonomic constraints of the superpotential at the string scale. This forbids the simultaneous presence of scalar fields and their complex conjugate. As an illustration, if the quantum numbers of H'' are those of N_R^c , then higher dimensional operators such as $\bar{N}_R N_R^c H''^2$, which can potentially generate a Majorana mass, are absent.² Because of holonomy this absence cannot be circumvented by including $\bar{N}_R N_R^c H''^{*2}$.

The scalar Lagrangian of SM^{++} is

$$\mathcal{L}_s^{++} = (\mathcal{D}^\mu H)^\dagger \mathcal{D}_\mu H + (\mathcal{D}^\mu H'')^\dagger \mathcal{D}_\mu H'' - V^{++}(H, H''), \quad (2)$$

² The identification of H'' with the superpartner of the right handed neutrino has been noted in [33].

TABLE I: Chiral spectrum of SM⁺⁺.

Fields	Sector	Representation	Q_B	Q_L	Q_{I_R}	Q_Y
U_R	$3 \rightleftharpoons 1^*$	(3, 1)	1	0	1	$\frac{2}{3}$
D_R	$3 \rightleftharpoons 1$	(3, 1)	1	0	-1	$-\frac{1}{3}$
L_L	$4 \rightleftharpoons 2$	(1, 2)	0	1	0	$-\frac{1}{2}$
E_R	$4 \rightleftharpoons 1$	(1, 1)	0	1	-1	-1
Q_L	$3 \rightleftharpoons 2$	(3, 2)	1	0	0	$\frac{1}{6}$
N_R	$4 \rightleftharpoons 1^*$	(1, 1)	0	1	1	0
H	$2 \rightleftharpoons 1$	(1, 2)	0	0	1	$\frac{1}{2}$
H''	$4 \rightleftharpoons 1$	(1, 1)	0	-1	-1	0

where

$$V^{++}(H, H'') = \mu_1^2 |H|^2 + \mu_2^2 |H''|^2 + \lambda_1 |H|^4 + \lambda_2 |H''|^4 + \lambda_3 |H|^2 |H''|^2 \quad (3)$$

is the potential and

$$\mathcal{D}_\mu = \partial_\mu - ig_3 T^a G_\mu^a - ig_3' Q_B C_\mu - ig_2 \tau^a W_\mu^a - ig_1' Q_{I_R} B_\mu - ig_4' Q_L X_\mu \quad (4)$$

is (in a self-explanatory notation [25]) the covariant derivative in the field basis shown in Fig. 1. Next, we impose the positivity conditions [34]

$$\lambda_1 > 0, \quad \lambda_2 > 0, \quad \lambda_1 \lambda_2 > \frac{1}{4} \lambda_3^2. \quad (5)$$

If the conditions (5) are satisfied, we can proceed to the minimisation of $V^{++}(H, H'')$ as a function of constant VEVs for the two Higgs fields. In the unitary gauge the fields can be written as

$$H \equiv \frac{1}{\sqrt{2}} \begin{pmatrix} 0 \\ v_1 + h_1(x) \end{pmatrix} \quad \text{and} \quad H'' \equiv \frac{1}{\sqrt{2}} (v_2 + h_2(x)), \quad (6)$$

with v_1 and v_2 real and non-negative. The physically most interesting solutions to the minimisation of (3) are obtained for v_1 and v_2 both non-vanishing

$$v_1^2 = \frac{-\lambda_2 \mu_1^2 + \frac{1}{2} \lambda_3 \mu_2^2}{\lambda_1 \lambda_2 - \frac{1}{4} \lambda_3^2} \quad \text{and} \quad v_2^2 = \frac{-\lambda_1 \mu_2^2 + \frac{1}{2} \lambda_3 \mu_1^2}{\lambda_1 \lambda_2 - \frac{1}{4} \lambda_3^2}. \quad (7)$$

To compute the scalar masses, we must expand the potential (3) around the minima (7). We denote by h and h'' the scalar fields of definite masses, m_h and $m_{h''}$, respectively. After a bit of algebra, the explicit expressions for the scalar mass eigenvalues and eigenvectors are given by

$$m_h^2 = \lambda_1 v_1^2 + \lambda_2 v_2^2 - \sqrt{(\lambda_1 v_1^2 - \lambda_2 v_2^2)^2 + (\lambda_3 v_1 v_2)^2}, \quad (8)$$

$$m_{h''}^2 = \lambda_1 v_1^2 + \lambda_2 v_2^2 + \sqrt{(\lambda_1 v_1^2 - \lambda_2 v_2^2)^2 + (\lambda_3 v_1 v_2)^2}, \quad (9)$$

$$\begin{pmatrix} h \\ h'' \end{pmatrix} = \begin{pmatrix} \cos \alpha & -\sin \alpha \\ \sin \alpha & \cos \alpha \end{pmatrix} \begin{pmatrix} h_1 \\ h_2 \end{pmatrix}, \quad (10)$$

where $\alpha \in [-\pi/2, \pi/2]$ also fullfills

$$\sin 2\alpha = \frac{\lambda_3 v_1 v_2}{\sqrt{(\lambda_1 v_1^2 - \lambda_2 v_2^2)^2 + (\lambda_3 v_1 v_2)^2}}, \quad (11)$$

$$\cos 2\alpha = \frac{\lambda_1 v_1^2 - \lambda_2 v_2^2}{\sqrt{(\lambda_1 v_1^2 - \lambda_2 v_2^2)^2 + (\lambda_3 v_1 v_2)^2}}. \quad (12)$$

Now, it is convenient to invert (8), (9) and (11), to extract the parameters in the Lagrangian in terms of the physical quantities m_h , $m_{h''}$ and $\sin 2\alpha$

$$\begin{aligned} \lambda_1 &= \frac{m_{h''}^2}{4v_1^2}(1 - \cos 2\alpha) + \frac{m_h^2}{4v_1^2}(1 + \cos 2\alpha), \\ \lambda_2 &= \frac{m_h^2}{4v_2^2}(1 - \cos 2\alpha) + \frac{m_{h''}^2}{4v_2^2}(1 + \cos 2\alpha), \\ \lambda_3 &= \sin 2\alpha \left(\frac{m_{h''}^2 - m_h^2}{2v_1 v_2} \right). \end{aligned} \quad (13)$$

One-loop corrections to (3) can be implemented by making λ_1 , λ_2 , and λ_3 field dependent quantities. Equation (5) then needs to be imposed in the regions where this is the case. When we talk about the stability of (3) at some energy Q (with the use of the couplings at that scale), we are thinking that the field values are at the scale Q . Note that the field values are the only physical quantities when talking about a potential like (3), and therefore the appropriate renormalization scale must also be at that scale. For $\lambda_3 > 0$ the third condition in (5) is only invalidated for field values v_1 around $m_{h''}$ regardless of the renormalization scale Q [35]. Namely, the instability region is given by

$$v_2 < \frac{m_{h''}}{\sqrt{2\lambda_2}}, \quad Q_- < v_1 < Q_+, \quad Q_{\pm}^2 = \frac{m_{h''}^2 \lambda_3}{8\lambda_1 \lambda_2} \left(1 \pm \sqrt{1 - \frac{4\lambda_1 \lambda_2}{\lambda_3^2}} \right) \Big|_{Q_*}, \quad (14)$$

where Q_* is some energy scale where the extra positivity condition is violated [35]. Thus, $Q_{\pm} \sim m_{h''}$ when the extra positivity condition is saturated, i.e. $\lambda_1 \lambda_2 = \lambda_3^2/4$. From (14) we see that $Q_{\pm} \sim m_{h''}$ when all the λ_i are roughly at the same scale. If one of the $\lambda_{1,2}$ is close to zero, then Q_+ can be $\gg m_{h''}$, but this region of the parameter space is taken care of by the condition $\lambda_{1,2} > 0$. The stability for field values at $m_{h''}$ is then determined by the potential with coupling at scale $m_{h''}$ (instead of Q). Therefore, for $\lambda_3 > 0$, we impose the extra positivity condition in the vicinity of $m_{h''}$. Even though the potential appears to be unstable at $Q \gg m_{h''}$, it is actually stable when all the field values are at the scale Q . Note that the potential with $\lambda_i(Q)$ can only be used when the physical quantities (field values v_1 , v_2) are at the scale Q . On the other hand, the instability region for $\lambda_3 < 0$ reads

$$v_2 > \frac{m_{h''}}{\sqrt{2\lambda_2}}, \quad c_- < \frac{v_1}{v_2} < c_+, \quad c_{\pm}^2 = -\frac{\lambda_3}{2\lambda_1} \left(1 \pm \sqrt{1 - \frac{4\lambda_1 \lambda_2}{\lambda_3^2}} \right) \Big|_{Q_*}, \quad (15)$$

and hence is given by the ratio of v_1 and v_2 , which can be reached even with both v_1 and v_2 being $\gg m_{h''}$ [35]. Therefore, for $\lambda_3 < 0$, we impose the extra positivity condition at all energy scales. Note that the asymmetry in λ_3 will carry over into an asymmetry in α .

As we noted above, the fields C_μ, X_μ, B_μ are related to Y_μ, Y'_μ, Y''_μ by an Euler rotation matrix [36],

$$\mathbb{R} = \begin{pmatrix} C_\theta C_\psi & -C_\phi S_\psi + S_\phi S_\theta C_\psi & S_\phi S_\psi + C_\phi S_\theta C_\psi \\ C_\theta S_\psi & C_\phi C_\psi + S_\phi S_\theta S_\psi & -S_\phi C_\psi + C_\phi S_\theta S_\psi \\ -S_\theta & S_\phi C_\theta & C_\phi C_\theta \end{pmatrix}. \quad (16)$$

Hence, the covariant derivative for the $U(1)$ fields in Eq. (4) can be rewritten in terms of Y_μ, Y'_μ , and Y''_μ as follows

$$\begin{aligned} \mathcal{D}_\mu &= \partial_\mu - iY_\mu (-S_\theta g'_1 Q_{I_R} + C_\theta S_\psi g'_4 Q_L + C_\theta C_\psi g'_3 Q_B) \\ &\quad - iY'_\mu [C_\theta S_\phi g'_1 Q_{I_R} + (C_\phi C_\psi + S_\theta S_\phi S_\psi) g'_4 Q_L + (C_\psi S_\theta S_\phi - C_\phi S_\psi) g'_3 Q_B] \\ &\quad - iY''_\mu [C_\theta C_\phi g'_1 Q_{I_R} + (-C_\psi S_\phi + C_\phi S_\theta S_\psi) g'_4 Q_L + (C_\phi C_\psi S_\theta + S_\phi S_\psi) g'_3 Q_B]. \end{aligned} \quad (17)$$

Now, by demanding that Y_μ has the hypercharge

$$Q_Y = c_1 Q_{I_R} + c_3 Q_B + c_4 Q_L \quad (18)$$

we fix the first column of the rotation matrix \mathbb{R}

$$\begin{pmatrix} C_\mu \\ X_\mu \\ B_\mu \end{pmatrix} = \begin{pmatrix} Y_\mu c_3 g_Y / g'_3 & \dots \\ Y_\mu c_4 g_Y / g'_4 & \dots \\ Y_\mu c_1 g_Y / g'_1 & \dots \end{pmatrix}, \quad (19)$$

and we determine the value of the two associated Euler angles

$$\theta = -\arcsin[c_1 g_Y / g'_1] \quad (20)$$

and

$$\psi = \arcsin[c_4 g_Y / (g'_4 C_\theta)], \quad (21)$$

with $c_1 = 1/2$, $c_3 = 1/6$, $c_4 = -1/2$, $B = Q_B/3$ and $L = Q_L$. The couplings g'_1 and g'_4 are related through the orthogonality condition, $P(g_Y, g'_1, g'_3, g'_4) = 0$, yielding

$$\left(\frac{c_4}{g'_4}\right)^2 = \frac{1}{g_Y^2} - \left(\frac{c_3}{g'_3}\right)^2 - \left(\frac{c_1}{g'_1}\right)^2, \quad (22)$$

with g'_3 fixed by the relation of $U(N)$ unification

$$g'_3(M_s) = \frac{1}{\sqrt{6}} g_3(M_s). \quad (23)$$

Next, by demanding that Y''_μ couples to an anomalous free linear combination of I_R and $B - L$ we determine the third Euler angle

$$\tan \phi = -S_\theta \frac{3 g'_3 C_\psi + g'_4 S_\psi}{3 g'_3 S_\psi - g'_4 C_\psi}. \quad (24)$$

The absence of abelian, mixed, and mixed gauge-gravitational anomalies is ensured utilizing the generalized Green-Schwarz mechanism, in which triangle anomalies are cancelled by Chern-Simons couplings. In the Y -basis we require the (mass)² matrix of the anomalous sector to be $\text{diag}(0, M'^2, 0)$. For the heavy field we take $M' \sim M_s$ and therefore $Y'_\mu \simeq Z'_\mu$ decouples from the low energy physics. The non-anomalous gauge boson, $Y''_\mu \simeq Z''_\mu$ grows a TeV-scale mass via H'' [25].

Altogether, the covariant derivative of the low energy effective theory reads

$$\mathcal{D}_\mu = \partial_\mu - ig_3 T^a G_\mu^a - ig_2 \tau^a W_\mu^a - ig_Y Q_Y Y_\mu - ig_y Q_Y Y''_\mu - ig_{B-L} (B-L) Y''_\mu, \quad (25)$$

where

$$\begin{aligned} g_Y &= -\frac{1}{2} S_\theta g'_1 = -\frac{1}{2} C_\theta S_\psi g'_4 = \frac{3}{2} C_\theta C_\psi g'_3 \\ g_y &= 2 C_\theta C_\phi g'_1 \\ g_{B-L} &= 3g'_3 (C_\phi C_\psi S_\theta + S_\phi S_\psi) - C_\theta C_\phi g'_1. \end{aligned} \quad (26)$$

Finally, a straightforward calculation leads to the RG equations for the five parameters in the scalar potential [37]

$$\begin{aligned} \frac{d\mu_1^2}{dt} &= \frac{\mu_1^2}{16\pi^2} \left(12\lambda_1 + 6Y_t^2 + 2\frac{\mu_2^2}{\mu_1^2} \lambda_3 - \frac{9}{2}g_2^2 - \frac{3}{2}g_Y^2 - \frac{3}{2}g_y^2 \right), \\ \frac{d\mu_2^2}{dt} &= \frac{\mu_2^2}{16\pi^2} \left(8\lambda_2 + 4\frac{\mu_1^2}{\mu_2^2} \lambda_3 - 24g_{B-L}^2 \right), \\ \frac{d\lambda_1}{dt} &= \frac{1}{16\pi^2} \left(24\lambda_1^2 + \lambda_3^2 - 6Y_t^4 + \frac{9}{8}g_2^4 + \frac{3}{8}g_Y^4 + \frac{3}{4}g_2^2 g_Y^2 + \frac{3}{4}g_2^2 g_y^2 + \frac{3}{4}g_Y^2 g_y^2 + \frac{3}{8}g_y^4 \right. \\ &\quad \left. + 12\lambda_1 Y_t^2 - 9\lambda_1 g_2^2 - 3\lambda_1 g_Y^2 - 3\lambda_1 g_y^2 \right), \\ \frac{d\lambda_2}{dt} &= \frac{1}{8\pi^2} (10\lambda_2^2 + \lambda_3^2 + 48g_{B-L}^4 - 24\lambda_2 g_{B-L}^2), \\ \frac{d\lambda_3}{dt} &= \frac{\lambda_3}{8\pi^2} \left(6\lambda_1 + 4\lambda_2 + 2\lambda_3 + 3Y_t^2 - \frac{9}{4}g_2^2 - \frac{3}{4}g_Y^2 - \frac{3}{4}g_y^2 - 12g_{B-L}^2 \right) + \frac{3}{4\pi^2} g_y^2 g_{B-L}^2, \end{aligned} \quad (27)$$

where $t = \ln Q$ and Y_t is the top Yukawa coupling, with

$$\frac{dY_t}{dt} = \frac{Y_t}{16\pi^2} \left(\frac{9}{2}Y_t^2 - 8g_3^2 - \frac{9}{4}g_2^2 - \frac{17}{12}g_Y^2 - \frac{17}{12}g_y^2 - \frac{2}{3}g_{B-L}^2 - \frac{5}{3}g_y g_{B-L} \right) \quad (28)$$

and $Y_t^{(0)} = \sqrt{2} m_t/v$. The RG running of the gauge couplings follow the standard form

$$\begin{aligned} \frac{dg_3}{dt} &= \frac{g_3^3}{16\pi^2} \left[-11 + \frac{4}{3}n_g \right] = -\frac{7}{16} \frac{g_3^3}{\pi^2}, \\ \frac{dg_2}{dt} &= \frac{g_2^3}{16\pi^2} \left[-\frac{22}{3} + \frac{4}{3}n_g + \frac{1}{6} \right] = -\frac{19}{96} \frac{g_2^3}{\pi^2}, \\ \frac{dg_Y}{dt} &= \frac{1}{16\pi^2} [A^{YY} g_Y^3], \\ \frac{dg_{B-L}}{dt} &= \frac{1}{16\pi^2} [A^{(B-L)(B-L)} g_{B-L}^3 + 2A^{(B-L)Y} g_{B-L}^2 g_y + A^{YY} g_{B-L} g_y^2], \\ \frac{dg_y}{dt} &= \frac{1}{16\pi^2} [A^{YY} g_y (g_y^2 + 2g_Y^2) + 2A^{(B-L)Y} g_{B-L} (g_y^2 + g_Y^2) + A^{(B-L)(B-L)} g_{B-L}^2 g_y], \end{aligned} \quad (29)$$

where $n_g = 3$ is the number of generations and

$$A^{ab} = A^{ba} = \frac{2}{3} \sum_f Q_{a,f} Q_{b,f} + \frac{1}{3} \sum_s Q_{a,s} Q_{b,s}, \quad (a, b = Y, B - L), \quad (30)$$

with f and s indicating contribution from fermion and scalar loops, respectively.

For energies below the mass of the heavier Higgs H'' , the effective theory is (of course) the SM. In the low energy regime the scalar Lagrangian then reads

$$\mathcal{L}_s = (\mathcal{D}^\mu H)^\dagger \mathcal{D}_\mu H - \mu^2 |H|^2 - \lambda |H|^4, \quad (31)$$

and the RG equations are those of SM. To obtain the matching conditions connecting the two theories, following [35] we integrate out the field H'' to obtain a Lagrangian of the form (31). Identifying the quadratic and quartic terms in the potential yields

$$\mu^2 = \mu_1^2 - \mu_2^2 \frac{\lambda_3}{2\lambda_2} \quad (32)$$

and

$$\lambda = \lambda_1 \left(1 - \frac{\lambda_3^2}{4\lambda_1\lambda_2} \right), \quad (33)$$

respectively. This is consistent with the continuity of $v \Leftrightarrow v_1$; namely

$$v^2 = - \frac{\mu^2}{\lambda} \Big|_{Q=m_{h''}} = - \frac{\mu_1^2 - \mu_2^2 \lambda_3 / (2\lambda_2)}{\lambda_1 [1 - \lambda_3^2 / (4\lambda_1\lambda_2)]} \Big|_{Q=m_{h''}}, \quad (34)$$

or equivalently

$$v^2 \Big|_{Q=m_{h''}} = v_1^2 \Big|_{Q=m_{h''}}, \quad (35)$$

with v_1 given by (7). The quartic interaction between the heavy scalar singlet and the Higgs doublet provides an essential contribution for the stabilization the scalar field potential [35].

III. RESULTS AND CONCLUSIONS

To ensure perturbativity of g'_4 between the TeV scale and the string scale we find from (22) that $g'_1 > 0.232$. We also take $g'_1 \lesssim 1$ in order to ensure perturbativity at the string scale. Let us first study the region of the parameter space constrained by $g'_1(M_s) \simeq 1$. The string-scale values of the other abelian couplings are fixed by previous considerations (22) and (23). The Euler angles at M_s are also fixed by (20), (21), and (24). All the couplings and angles are therefore determined at all energies through RG running. As an illustration we set $M_s = 10^{14}$ GeV; this leads to $g'_3(M_s) = 0.231$, $g'_4(M_s) = 0.232$, $\psi(M_s) = -1.245$, $\theta(M_s) = -0.217$, and $\phi(M_s) = -0.0006$. Next, we define $Q_{\min} = 125$ GeV and normalize $t = \ln(Q/125 \text{ GeV})$ and $t_{\max} = \ln(\Lambda/125 \text{ GeV})$. Finally, we run the couplings and angles down to the TeV region: $g'_1 = 0.406$, $g'_3 = 0.196$, $g'_4 = 0.218$, $\theta = -0.466$, $\psi = -1.215$, and $\phi = -0.0003$.

Using the SM relation $m_H^2 = -2\mu^2$, with $m_H \simeq 125$ GeV, and setting $v^2 = 246$ GeV at the same energy scale $Q = 125$ GeV fixes the initial conditions for the parameters μ and λ . It should be noted that we take the top Yukawa coupling evaluated at m_t . This introduces

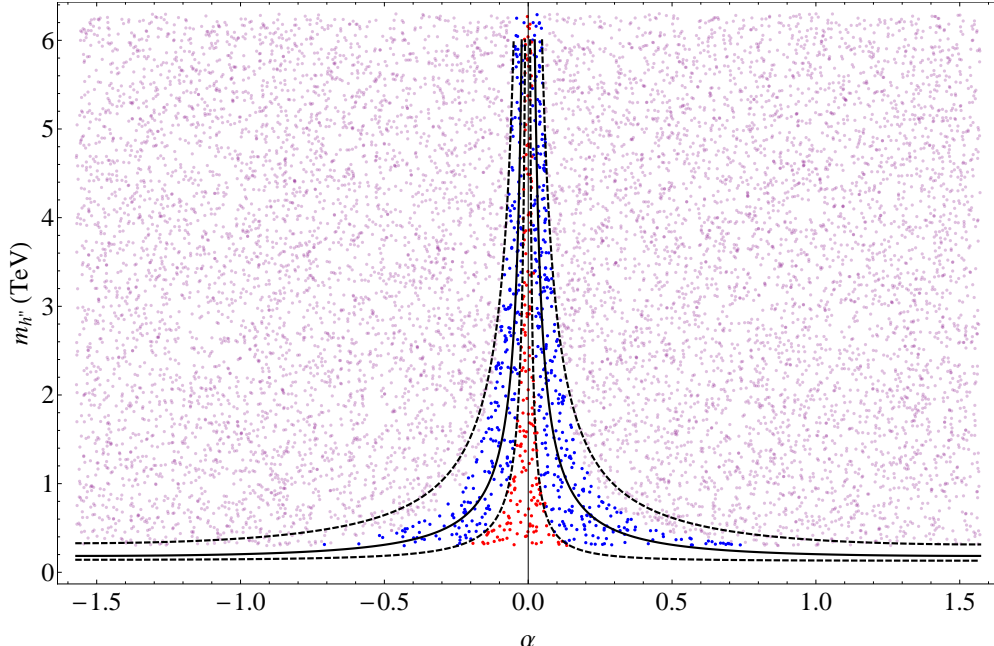


FIG. 2: An exhibition of the SM⁺⁺ vacuum stability patterns in the $m_{h''}$ vs α plane, for $M_{Z''} = 4.5$ TeV. The analysis is based on a scan of 10^4 trial random points with $M_s = 10^{14}$ GeV. The points yielding a stable vacuum solution up to M_s are blue-printed, those leading to unstable vacuum solutions are red-printed, and points giving runaway solutions (*i.e.*, those in which the Higgs doublet self-coupling blows up) are purple-printed. Fits to the boundaries defining the region with stable vacuum solutions (dashed lines) and to the average value of the scatter points contained in that region (solid lines) are also shown.

a small unnoticeable error. On the other hand, m_t is taken to be the physical top mass. Have we used the running mass instead as in [38], the running of the quartic coupling λ would become much slower, with the instability scale pushed to almost 10^9 GeV. We run the SM couplings from 125 GeV up to the mass scale $m_{h''}$ and use the matching conditions to determine v , which in turns allows one to solve algebraically for m_h .

After completing this task, there are *a priori* three free parameters to be fixed at the TeV-scale: $(v_2, \alpha, m_{h''})$. The initial values of g_Y , g_γ and g_{B-L} are then fixed by previous considerations (26). Actually, using the relation $M_{Z''} = g'_1 C_\phi v_2 / C_\theta$ [25], we adopt $(M_{Z''}, \alpha, m_{h''})$ as the free parameters of the model.³ For $M_s = 10^{14}$ GeV, we perform a scan of 10^4 trial random set of points, $(M_{Z''}, \alpha, m_{h''})$, and using (13) we obtain the initial conditions $(\lambda_1^{(0)}, \lambda_2^{(0)}, \lambda_3^{(0)})$ to integrate (27). For each set of points, we verify that the positivity condition (5) is fulfilled all the way to $\Lambda = M_s$. The 10^4 trials are duplicated for $M_s = 10^{16}$ and $M_s = 10^{19}$ GeV. Our results are encapsulated in Figs. 2 to 8, and along with other aspects of this work are summarized in these concluding remarks:

- In Fig. 2 we show the entire scan for $M_s = 10^{14}$ GeV and $M_{Z''} = 4.5$ TeV. The

³ For $M_s = 10^{14}$ GeV, the $v_2 \simeq M_{Z''}$ relation implies that if $7 \text{ TeV} < v_2 < 13 \text{ TeV}$, then $3.2 \text{ TeV} < M_{Z''} < 6.0 \text{ TeV}$. For a different M_s the range of $M_{Z''}$ is altered because of changes in g'_1 , θ , and ϕ ; *e.g.* for $M_s = 10^{19}$ GeV, the range becomes $2.8 \text{ TeV} < M_{Z''} < 5.8 \text{ TeV}$.

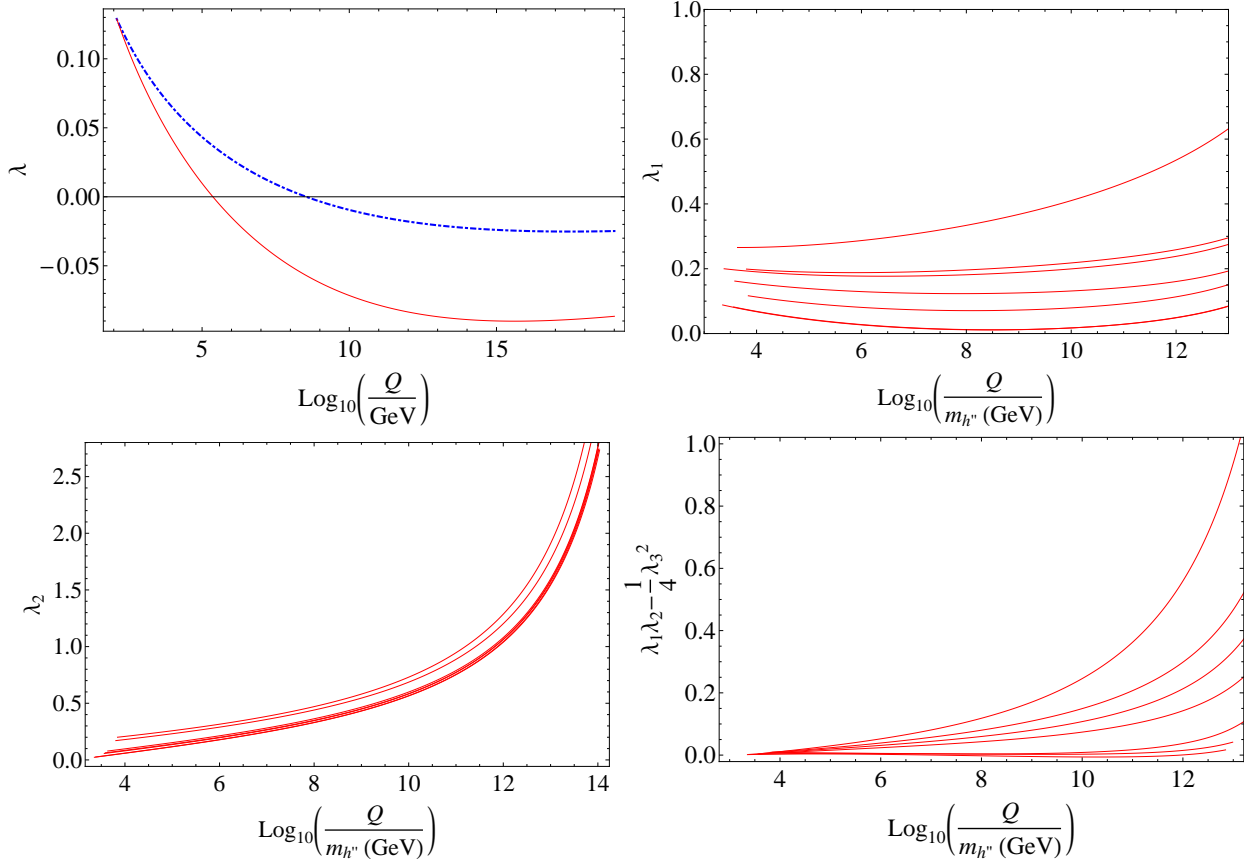


FIG. 3: From left to right downwards: the first panel shows the running of λ from its value at 125 GeV (red solid line $m_t = 172.9$ GeV and blue dot-dashed line $m_t = 164$ GeV); the second and third panels show the typical behavior of the running couplings $\lambda_1(t)$ and $\lambda_2(t)$ for the average value of the initial condition, $\langle \lambda_1^{(0)} \rangle = 0.28$ in the integration of (27); the fourth panel shows the behavior of the extra positivity condition for $\alpha < 0$. In the running of λ_i we have taken $M_s = 10^{14}$ GeV.

points yielding a stable vacuum solution up to M_s are blue-printed, those leading to unstable vacuum solutions are red-printed, and points giving runaway solutions are purple-printed. A stable vacuum solution is one in which the positivity condition (5) is fulfilled all the way to $\Lambda = M_s$. An unstable solution is one in which the stability conditions of the vacuum ($\lambda_1 > 0$, $\lambda_2 > 0$, $\lambda_1\lambda_2 > \lambda_3^2/4$) are violated. (Recall that for the case $\lambda_3 > 0$ there is no need to impose the third condition in (5) at all scales, but only in the vicinity of $m_{h''}$.) A runaway solution is one in which the RG equations drive the Higgs doublet self-coupling non-perturbative. The perturbative upper bound (sometimes referred to as ‘triviality’ bound) is given by $\lambda_1 < 2\pi$ at any point in the RG evolution [20]. The vacuum stability condition is driven by the behavior of λ_1 , and actually is largely dominated by the initial condition $\lambda_1^{(0)}$. Indeed, if the extra gauge boson Z'' gets its mass through a non-Higgs mechanism and the scalar potential (3) is that of SM (*i.e.* $v_2 = \lambda_2 = \lambda_3 = 0$), the RG evolution collapses to that of SM and there are no stable solutions.⁴

⁴ Of course, even if $v_2 = \lambda_2 = \lambda_3 = 0$, with an extra gauge boson the RG evolution of λ_1 is not exactly

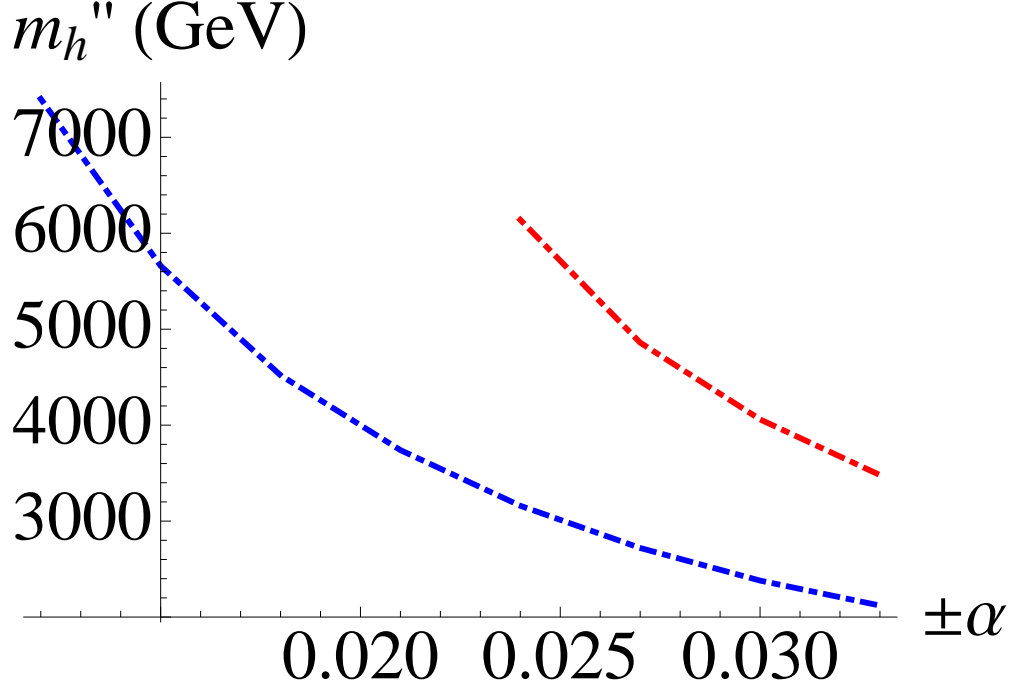


FIG. 4: The lower boundary of the allowed parameter space in the $m_{h''} - \alpha$ plane under the vacuum stability constraint of Eq. (5), for the positive alpha (blue) and negative alpha (red). We have taken $M_{Z''} = 4.5$ TeV and $M_s = 10^{14}$ GeV.

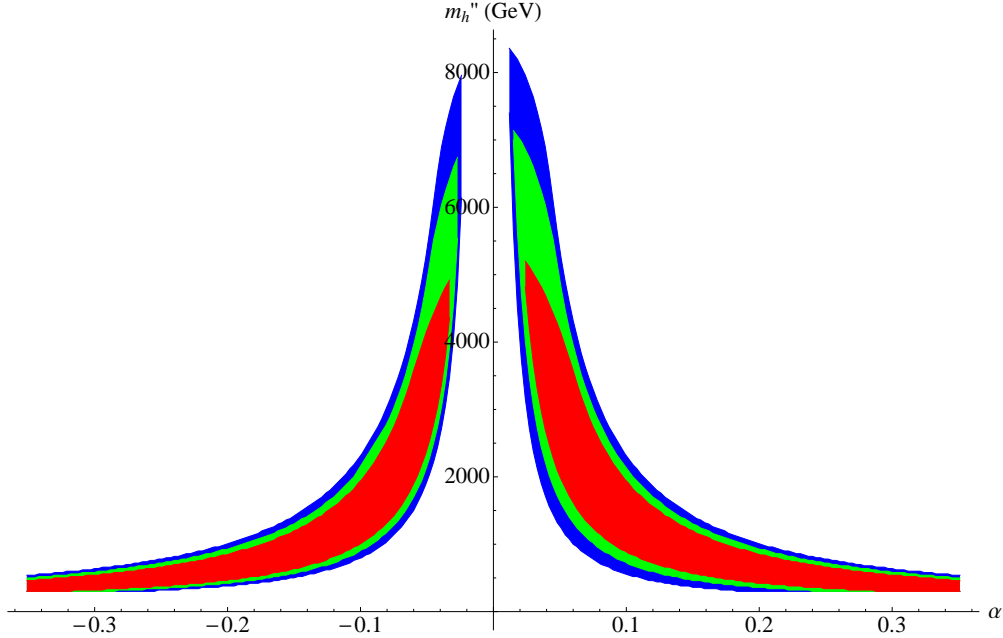


FIG. 5: The allowed SM^{++} parameter space in the $m_{h''}$ vs α plane under the vacuum stability constraint of Eq. (5), for the case $M_{Z''} = 4.5$ TeV, with $M_s = 10^{14}$ GeV (blue), $M_s = 10^{16}$ GeV (green), and $M_s = 10^{19}$ GeV (red). The perturbative upper bound is defined by $\lambda_i < 2\pi$.

that of SM, see (27).

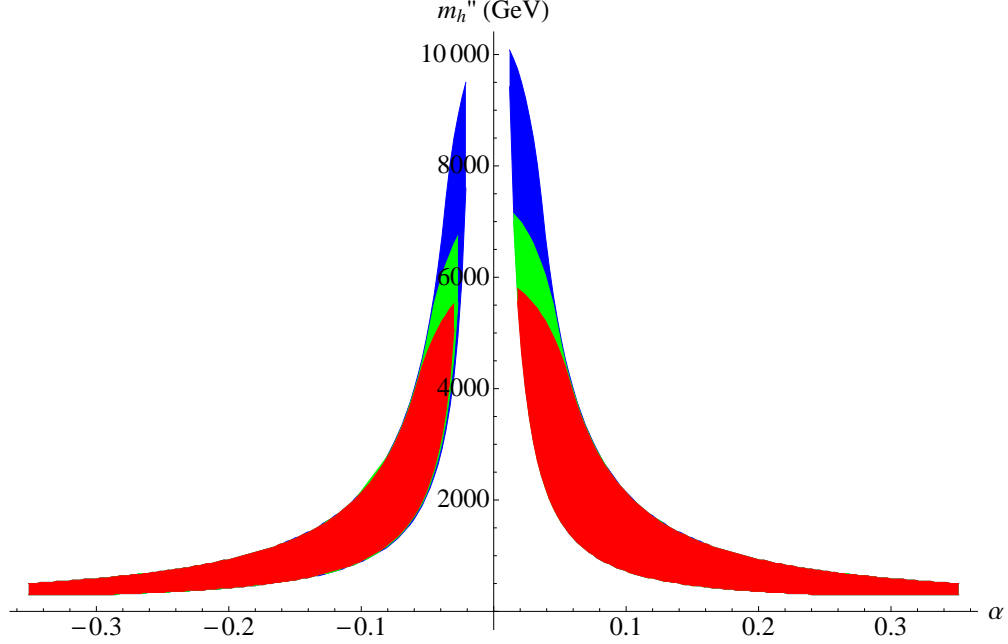


FIG. 6: Variation of SM^{++} vacuum stability regions with $M_{Z''}$. We have taken $M_s = 10^{16}$ GeV, $M_{Z''} = 3.5$ TeV (red), $M_{Z''} = 4.5$ TeV (green), and $M_{Z''} = 6.0$ TeV (blue). The perturbative upper bound is defined by $\lambda_i < 2\pi$.

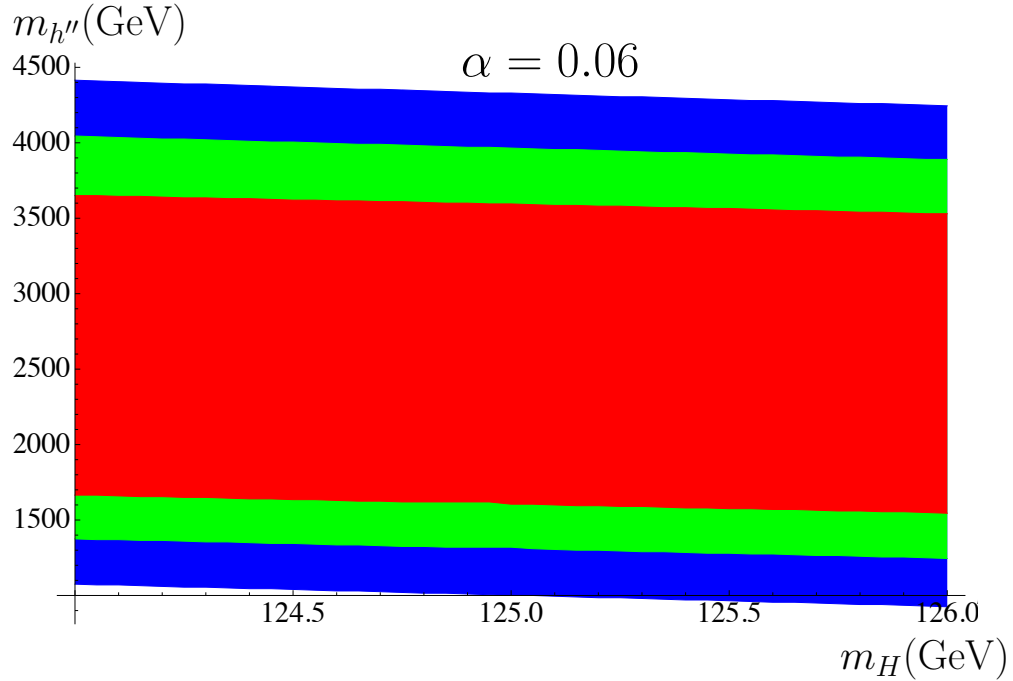


FIG. 7: Variation of SM^{++} vacuum stability regions with m_H . We have taken $\alpha = 0.06$, $M_{Z''} = 4.5$ TeV, $M_s = 10^{14}$ GeV (blue), $M_s = 10^{16}$ GeV (green), $M_s = 10^{19}$ GeV (red). The perturbative upper bound is defined by $\lambda_i < 2\pi$.

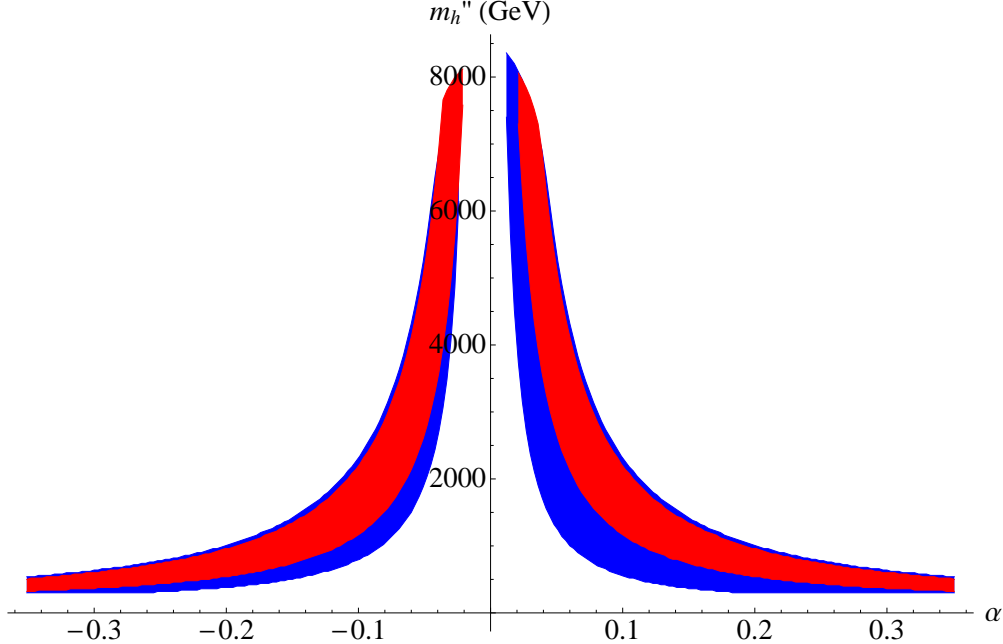


FIG. 8: Variation of SM^{++} vacuum stability regions with $g'_1(M_s)$. The stable regions correspond to $g'_1(M_s) = 1.000$ (blue), $g'_1(M_s) = 0.232$ (red). We have taken $M_s = 10^{14}$ GeV, $M_{Z''} = 4.5$ TeV, $m_H = 125$ GeV. The perturbative upper bound is defined by $\lambda_i < 2\pi$.

- To determine the range of initial conditions $\lambda_1^{(0)}$ yielding stable vacuum solutions we fit the boundaries of the blue band in the scatter plot. The resulting curves, which are shown as dashed lines in Fig. 2, correspond to $0.16 < \lambda_1^{(0)} < 0.96$ for $\alpha < 0$ and $0.15 < \lambda_1^{(0)} < 0.96$ for $\alpha > 0$. The lower limit of $\lambda_1^{(0)}$, which defines the boundary between stable and unstable solutions, is close to the value required for vacuum stability of the SM potential, as shown in (1). Namely, substituting $m_h = 130$ GeV and $\alpha = 0$ in (13) we obtain $\lambda_1^{(0)} = 0.14$. The similarities between the minimum value of m_H that allows absolute stability up to the Planck scale within SM and the minimum value of m_h in the decoupling limit of (13) reinforces our previous statement concerning the strong dependence of the RG evolution with the initial condition $\lambda_1^{(0)}$. We have also determined the average value of the initial condition $\lambda_1^{(0)}$ through a fit to the blue points in the scattered plot. The result, which is shown as a solid lines in Fig. 2, corresponds to $\langle \lambda_1^{(0)} \rangle = 0.28$. The behavior of λ together with the typical behavior of λ_1 and λ_2 for the average value of the initial condition $\langle \lambda_1^{(0)} \rangle$, are shown in Fig. 3. Note that λ_1 heads towards the instability and reaches a minimum greater than zero; thereafter rises towards the Landau point. This behavior is characteristic of models with scalar singlets [39]. We also show in Fig. 3 the typical behavior of $\lambda_1\lambda_2 - \lambda_3^2/4$ for $\alpha < 0$ and $\langle \lambda_1^{(0)} \rangle = 0.28$.
- Even though the asymmetry between $\pm\alpha$ appears to be small on Fig. 2, it is not actually insignificant. In fact, for a given α , the lower boundary sometimes changes by a factor of two. For example, at $\alpha = 0.24$, it changes from 6,140 GeV to 3,160 GeV. However, the effect on the area is less noticeable. The reason is that we can only change the lower boundaries of the accepted parameter space. The upper boundary

is determined by the constraint that λ_i (usually λ_2) remains perturbative. This constraint is symmetric with respect to α . So the area cannot be enlarged indefinitely. Even if somehow we can send the lower boundary to zero, the area would only increase by another 20% to 30%. The asymmetry becomes more obvious if we only consider the lower boundary, as shown in Fig. 4.

- To determine the sensitivity of the RG evolution with respect to the choice of the string scale, we duplicate the analysis for $M_s = 10^{16}$ GeV and $M_s = 10^{19}$ GeV. The contours display in Fig. 5 (for $M_{Z''} = 4.5$ TeV) show that the region of stable vacuum solutions shrinks as M_s increases. The allowed range of initial conditions with stable vacuum solutions therefore depends on the value of the string scale; *e.g.* for $M_s = 10^{16}$ GeV, we obtain $0.17 < \lambda_1^{(0)} < 0.83$ for $\alpha < 0$ and $0.16 < \lambda_1^{(0)} < 0.83$ for $\alpha > 0$, whereas for $M_s = 10^{19}$ GeV, we obtain $0.18 < \lambda_1^{(0)} < 0.69$ for $\alpha < 0$ and $0.17 < \lambda_1^{(0)} < 0.69$ for $\alpha > 0$. The corresponding average value for $M_s = 10^{16}$ GeV is $\langle \lambda_1^{(0)} \rangle = 0.31$, and for $M_s = 10^{19}$ GeV is $\langle \lambda_1^{(0)} \rangle = 0.32$.
- In Fig. 6 we display the sensitivity of the RG evolution with $M_{Z''}$. For large values of $|\alpha|$ there is no variation in the contour regions. For $\alpha \gtrsim -0.05$ and $\alpha \lesssim 0.06$ there are some small variances. This small differences show the effect of the initial conditions $\lambda_2^{(0)}$ and $\lambda_3^{(0)}$ (both depending directly on $M_{Z''}$) on the evolution of the system.
- We have verified that there is no significant variation of the SM⁺⁺ vacuum stability regions within the m_H uncertainty. An example for $\alpha = 0.06$ and $M_{Z''} = 4.5$ TeV is given in Fig. 7.
- In Fig. 8 we display the variation of our results with $g'_1(M_s)$. It is clearly seen that for $0.232 < g'_1(M_s) < 1.000$ the dependence on g'_1 seems to be fairly weak. The stability of SM⁺⁺ vacuum is then nearly independent of the Z'' branching fractions [25].
- The low energy effective theory discussed in this paper requires a high level of fine tuning, which is satisfyingly resolved by applying the anthropic landscape of string theory [40–42]. Alternatively, the fine tuning can be circumvented with a more complete broken SUSY framework. Since in pure SUSY the vacuum is automatically stable, the stability analysis perforce involves the soft SUSY-breaking sector. Hence rather than simply searching for the Higgs self-coupling going negative in the ultraviolet, the stability analysis would involve finding the local and global minima of the effective potential in the multi-dimensional space of the soft-breaking sector [43]. However, the Higgs mass range favored by recent LHC data may be indicative of high-scale SUSY breaking [44]; perhaps near the high energy cutoff of the field theory, beyond which a string description becomes a necessity [45].

In summary, we have shown that SM⁺⁺ is a viable low energy effective theory, with a well-defined range of free parameters.

Acknowledgments

L.A.A. and BV are supported by the U.S. National Science Foundation (NSF) under CAREER Grant PHY-1053663. I.A. is supported in part by the European Commission

under the ERC Advanced Grant 226371 and the contract PITN-GA-2009- 237920. H.G. and T.R.T. are supported by NSF Grant PHY-0757959. X.H. is supported in part by the National Research Foundation of Korea grants 2005-009-3843, 2009-008-0372, and 2010-220-C00003. D.L. is partially supported by the Cluster of Excellence "Origin and Structure of the Universe", in Munich. D.L. and T.R.T. thank the Theory Department of CERN for its hospitality. L.A.A. and H.G. thank the Galileo Galilei Institute for Theoretical Physics for the hospitality and the INFN for partial support during the completion of this work. Any opinions, findings, and conclusions or recommendations expressed in this material are those of the authors and do not necessarily reflect the views of the National Science Foundation.

-
- [1] F. Gianotti, CERN Seminar: *Update on the Standard Model Higgs Searches in ATLAS*, July 4, 2012.
 - [2] J. Incandela, CERN Seminar: *Update on the Standard Model Higgs Searches in CMS*, July 4, 2012.
 - [3] G. Aad *et al.* [ATLAS Collaboration], Phys. Lett. B **710**, 49 (2012) [arXiv:1202.1408 [hep-ex]].
 - [4] S. Chatrchyan *et al.* [CMS Collaboration], arXiv:1202.1488 [hep-ex].
 - [5] O. Arnaez (on behalf of the ATLAS Collaboration), *Searches for the SM scalar boson in the $H \rightarrow W^+W^-$ channels with the ATLAS detector*, talk given at Higgs Hunting 2012, Orsay, France, 18-20 July, 2012.
 - [6] G. Aad *et al.* [ATLAS Collaboration], arXiv:1207.7214 [hep-ex].
 - [7] S. Chatrchyan *et al.* [CMS Collaboration], arXiv:1207.7235 [hep-ex].
 - [8] T. Aaltonen *et al.* [CDF and D0 Collaborations], arXiv:1207.6436 [hep-ex].
 - [9] P. P. Giardino, K. Kannike, M. Raidal and A. Strumia, arXiv:1207.1347 [hep-ph].
 - [10] J. R. Espinosa, C. Grojean, M. Muhlleitner and M. Trott, arXiv:1207.1717 [hep-ph].
 - [11] T. Plehn and M. Rauch, arXiv:1207.6108 [hep-ph].
 - [12] M. Lindner, M. Sher and H. W. Zaglauer, Phys. Lett. B **228**, 139 (1989).
 - [13] M. Sher, Phys. Rept. **179**, 273 (1989).
 - [14] M. A. Diaz, T. A. ter Veldhuis and T. J. Weiler, Phys. Rev. Lett. **74**, 2876 (1995) [hep-ph/9408319].
 - [15] J. A. Casas, J. R. Espinosa and M. Quiros, Phys. Lett. B **342**, 171 (1995) [hep-ph/9409458].
 - [16] M. A. Diaz, T. A. ter Veldhuis and T. J. Weiler, Phys. Rev. D **54**, 5855 (1996) [hep-ph/9512229].
 - [17] J. A. Casas, J. R. Espinosa and M. Quiros, Phys. Lett. B **382**, 374 (1996) [hep-ph/9603227].
 - [18] G. Isidori, G. Ridolfi and A. Strumia, Nucl. Phys. B **609**, 387 (2001) [hep-ph/0104016].
 - [19] G. Isidori, V. S. Rychkov, A. Strumia and N. Tetradis, Phys. Rev. D **77**, 025034 (2008) [arXiv:0712.0242 [hep-ph]].
 - [20] J. Ellis, J. R. Espinosa, G. F. Giudice, A. Hoecker and A. Riotto, Phys. Lett. B **679**, 369 (2009) [arXiv:0906.0954 [hep-ph]].
 - [21] J. Elias-Miro, J. R. Espinosa, G. F. Giudice, G. Isidori, A. Riotto and A. Strumia, Phys. Lett. B **709**, 222 (2012) [arXiv:1112.3022 [hep-ph]].
 - [22] Z. -z. Xing, H. Zhang and S. Zhou, arXiv:1112.3112 [hep-ph].
 - [23] F. Bezrukov, M. Y. Kalmykov, B. A. Kniehl and M. Shaposhnikov, arXiv:1205.2893 [hep-ph].
 - [24] G. Degrandi, S. Di Vita, J. Elias-Miro, J. R. Espinosa, G. F. Giudice, G. Isidori and A. Strumia, arXiv:1205.6497 [hep-ph].

- [25] L. A. Anchordoqui, I. Antoniadis, H. Goldberg, X. Huang, D. Lüüst, T. R. Taylor and B. Vlleck, arXiv:1206.2537 [hep-ph].
- [26] D. Lüüst, *Class. Quant. Grav.* **21** (2004) S1399 [hep-th/0401156].
- [27] R. Blumenhagen, M. Cvetic, P. Langacker and G. Shiu, *Ann. Rev. Nucl. Part. Sci.* **55**, 71 (2005) [arXiv:hep-th/0502005].
- [28] R. Blumenhagen, B. Körs, D. Lüüst, S. Stieberger, *Phys. Rept.* **445**, 1 (2007) [hep-th/0610327].
- [29] D. Cremades, L. E. Ibanez and F. Marchesano, *JHEP* **0307**, 038 (2003) [hep-th/0302105].
- [30] L. A. Anchordoqui, I. Antoniadis, H. Goldberg, X. Huang, D. Lüüst and T. R. Taylor, *Phys. Rev. D* **85**, 086003 (2012) [arXiv:1107.4309 [hep-ph]].
- [31] D. Berenstein and S. Pinansky, *Phys. Rev. D* **75**, 095009 (2007) [hep-th/0610104].
- [32] M. Cvetic, J. Halverson and P. Langacker, *JHEP* **1111**, 058 (2011) [arXiv:1108.5187 [hep-ph]].
- [33] M. Kadastik, K. Kannike and M. Raidal, *Phys. Rev. D* **80**, 085020 (2009) [Erratum-ibid. *D* **81**, 029903 (2010)] [arXiv:0907.1894 [hep-ph]].
- [34] V. Barger, P. Langacker, M. McCaskey, M. Ramsey-Musolf and G. Shaughnessy, *Phys. Rev. D* **79**, 015018 (2009) [arXiv:0811.0393 [hep-ph]].
- [35] J. Elias-Miro, J. R. Espinosa, G. F. Giudice, H. M. Lee and A. Strumia, *JHEP* **1206**, 031 (2012) [arXiv:1203.0237 [hep-ph]].
- [36] L. A. Anchordoqui, H. Goldberg, X. Huang, D. Lüüst and T. R. Taylor, *Phys. Lett. B* **701**, 224 (2011) [arXiv:1104.2302 [hep-ph]].
- [37] L. Basso, S. Moretti and G. M. Pruna, *Phys. Rev. D* **82**, 055018 (2010) [arXiv:1004.3039 [hep-ph]].
- [38] J. A. Casas, J. R. Espinosa, M. Quiros and A. Riotto, *Nucl. Phys. B* **436**, 3 (1995) [Erratum-ibid. *B* **439**, 466 (1995)] [hep-ph/9407389].
- [39] M. Kadastik, K. Kannike, A. Racioppi and M. Raidal, *JHEP* **1205**, 061 (2012) [arXiv:1112.3647 [hep-ph]].
- [40] R. Bousso and J. Polchinski, *JHEP* **0006**, 006 (2000) [hep-th/0004134].
- [41] L. Susskind, [hep-th/0302219].
- [42] M. R. Douglas, *JHEP* **0305**, 046 (2003) [hep-th/0303194].
- [43] M. Claudson, L. J. Hall and I. Hinchliffe, *Nucl. Phys. B* **228**, 501 (1983).
- [44] L. J. Hall and Y. Nomura, *JHEP* **1003**, 076 (2010) [arXiv:0910.2235 [hep-ph]].
- [45] A. Hebecker, A. K. Knochel and T. Weigand, *JHEP* **1206**, 093 (2012) [arXiv:1204.2551 [hep-th]].